

Time Series Anomaly Detection With Adversarial Reconstruction Networks

Shenghua Liu^{ID}, Bin Zhou, Quan Ding^{ID}, Bryan Hooi, Zhengbo Zhang, Huawei Shen^{ID}, and Xueqi Cheng

Abstract—Time series data naturally exist in many domains including medical data analysis, infrastructure sensor monitoring, and motion tracking. However, a very small portion of anomalous time series can be observed, comparing to the whole data. Most existing approaches are based on the supervised classification model requiring representative labels for anomaly class(es), which is challenging in real-world problems. So can we learn how to detect anomalous time ticks in an effective yet efficient way, given mostly normal time series data? Therefore, we propose an unsupervised reconstruction model named BeatGAN which learns to detect anomalies based on normal data, or data which majority of samples are normal. BeatGAN provides a framework to adversarially learn to reconstruct, which can cooperate with both 1-d CNN and RNN. Rarely observed anomalies can result in larger reconstruction errors, which are then detected based on extreme value theory. Moreover, data augmentation with dynamic time warping regularizes reconstruction and provides robustness. In the experiments, effectiveness and sensitivity are studied in both synthetic data and various real-world time series. BeatGAN achieves better accuracy and fast inference.

Index Terms—Time series, adversarial reconstruction networks, anomaly detection, data augmentation

1 INTRODUCTION

TIME series is an important type of data object, which has the characteristics of high dimensions, large data volume, and real-time streaming, and it is widely used in various applications. For example, in the medical field, the patient's ECG data and respiratory data are recorded through medical equipment. In the industrial field, sensors of various devices collect state data in real time. In the financial field, exchanges record stock price changes every moment which form time series data. These massive time series data contain various information, and some of them are different from the general mode of the data, and their characteristics are obviously different from most data. We call such data "anomalous data", which Fig. 1 shows an example in ECG waveform. Although the proportion of anomalous data is very small, it often contains more valuable information and has important research value in various fields. For example, in the medical field, patients have a large amount of monitoring data such as

electrocardiogram, blood pressure, respiration rate, etc. Using these data to detect the abnormal state of the patient and early warning is the primary goal of modern medical treatment. So, it is very significant to propose a method detecting anomalous time series segments in large-scale rhythmic time series data.

Another key goal in our research is explainability. In practice, experts in medical and other domains need to know not only whether an anomaly exists but also to understand the mechanism of anomalies. This leads to the following questions:

How can we automatically detect anomalous beats when monitoring multivariate time series? Can we pinpoint the anomalous time ticks that led to our decision?

The traditional anomaly detection algorithm faces the shortcomings of low efficiency and shallow accuracy in today's massive and complex data, and cannot model the characteristics of normal samples precisely. Besides, there are several challenges in time series anomaly detection: 1) massive time series can contain few anomalies, which is insufficient and imbalanced for supervised classification; 2) anomalous segments can be very different from one another, e.g., some anomalous heartbeats are never seen in defined categories; 3) even in healthy patients, the time periods involved in various heartbeat characteristics (e.g., P waves, QRS complex, P-R, and R-R intervals) vary from one beat to another.

Different from supervised methods, unsupervised anomaly detection methods are trained only on *normal* samples, and then used to identify *abnormal* samples. Among many anomaly detection methods, reconstruction-based anomaly detection techniques are widely used. We expect to obtain the true nature of the data by reconstructing them with their lower-dimensional representation, then the reconstruction error can be measured as the anomaly score for given samples. [1] uses reconstruction error between true and latent representation to detect anomalies by the modified SVD

- Shenghua Liu, Bin Zhou, Quan Ding, Huawei Shen, and Xueqi Cheng are with the Institute of Computing Technology, Chinese Academy of Sciences, Beijing 100045, China, and also with the University of Chinese Academy of Sciences, Beijing 101408, China. E-mail: liu.shengh@gmail.com, {zhoubin17g, shenhuawei, cxq}@ict.ac.cn, dingquan@mail.nankai.edu.cn.
- Bryan Hooi is with the School of Computer Science, National University of Singapore, Singapore 119077. E-mail: dcsbhk@nus.edu.sg.
- Zhengbo Zhang is with the Center for Artificial Intelligence in Medicine, Chinese PLA General Hospital, Beijing 100010, China. E-mail: zhengbozhang@126.com.

Manuscript received 28 July 2020; revised 31 August 2021; accepted 23 December 2021. Date of publication 4 January 2022; date of current version 7 March 2023.

This work was supported in part by the National Science Foundation of China under Grants U1911401, 91746301, 61772498, 61872206 and U21B2046, and part by the Strategic Priority Research Program of the Chinese Academy of Sciences under Grant XDA19020400.

(Corresponding author: Shenghua Liu.)

Recommended for acceptance by K.S. Candan.

Digital Object Identifier no. 10.1109/TKDE.2021.3140058

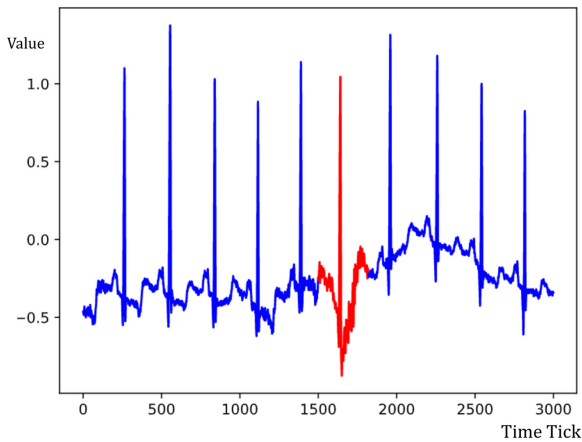


Fig. 1. ECG waveform data with anomalies.

decomposition. Autoencoder (AE) [2] allows for more complex patterns by applying nonlinear functions for reconstruction and anomaly detection. However, without proper regularization, such a reconstruction easily leads to overfitting, resulting in low accuracy.

Generative adversarial networks (GANs) is a successful generative model that jointly learns to generate realistic synthetic data while learning a discriminator [3]. Some works utilize both generator and discriminator [4] for anomaly detection and it provides an intuitive way to regularize the reconstruction error.

Therefore, we propose an anomaly detection model, *BeatGAN*, which detects anomalies using adversarially generated time series as shown in Fig. 2. The model additionally provides explainable results, pinpointing the time ticks that led to our decision, rather than just an overall anomalousness score.

BeatGAN reconstructs the data robustly and performs regularization using an adversarial generation approach. The generation is fulfilled by reconstruction and regularization of jointly optimizing hidden feature matching and discrimination in a generative adversarial network. Pairwise feature matching loss and the reconstruction loss are used to tune model parameters. To further improve its accuracy, we exploit the characteristics of rhythmic time series by designing a warping method to augment training data in our proposed *BeatGAN* method. Experiments show that *BeatGAN* detects anomalies accurately in different types of time series like ECG data from the MIT-BIH arrhythmia database, multivariate time series from SWaT database, and sensor time series data from the CMU Motion Capture database.

In summary, our main contributions are as follows:

- *Anomaly detection by observing massive normal time series*: We propose to use a reconstruction-error method with the generative adversary network, named *BeatGAN* to detect anomalous time series, by comparing the difference between generated time series and the original one. Taking advantage of adversarial regularization, *BeatGAN* is robust. Moreover, time series warping is proposed for data augmentation to improve detection accuracy.
- *Effectiveness*: *BeatGAN* outperforms existing state-of-the-art methods in identifying anomalies in ECG

and SWaT time series, achieving an accuracy of nearly 0.95 and 0.82 AUC, and very fast inference (2.6 ms per beat).

- *Explainability*: *BeatGAN* is capable of pinpointing where the anomalous patterns occur, outputting interpretable results by visualization and attention routing (see Fig. 2).
- *Generality*: *BeatGAN* can successfully detect anomalies from the different multivariate sensor time series databases.
- *Reproducibility*: *BeatGAN* is open-sourced.¹

The rest of the paper is organized as follows. Section 2 summarizes the related works about anomaly detection. In Section 3, we describe the key components of our *BeatGAN* framework, and the corresponding optimization algorithm. In Section 4, we design our experiments with several datasets and analysis the results. Section 5 presents the conclusions.

2 RELATED WORK

Time series mining and anomaly detection methods can be categorized into four categories.

2.1 Statistics-Based Methods

Statistical-based methods mainly identify abnormal points that deviate from the normal distribution. A classical statistics-based method is 3-sigma criterion [5], which assumes that the data follows a normal distribution, and then the probability that the data is within the 3-sigma range ($\mu - 3\sigma, \mu + 3\sigma$) is 99.74%. Then the data that falls outside this interval is regarded as anomalous data. Besides, the Grubbs' test [6] is a statistical-based method as well. It also assumes the data follows a normal distribution and can output the confidence of each test sample. These methods require a prior assumption while real world data may not satisfy. So some works use the extreme value theory to detect the anomalies in univariable time series [7], [8]. This method doesn't need to assume the prior distribution of the data, but it still can not handle the multivariable time series well.

2.2 Classification-Based Methods

Supervised classification approaches require a large amount of labeled data, and either manually defined features or hidden variables learned from deep models. If given enough labeled data, these deep learning based approaches can achieve high accuracy [9], [10], [11]. However, the labeled data is usually difficult to obtain in practice [12]. Furthermore, it has difficulty generalizing to anomalies which differ significantly from those it has seen, e.g., when new types of anomalies appear. Based on these defects, Scholkopf proposed One-Class SVM [13], an unsupervised model which learns from normal data to identify anomalies on unseen data. It works by separating the origin from the data instances in a kernel space, corresponding to nonlinear regions describing the normal data in feature space. Each instance's anomalousness score is measured by its normalized distance to the determined decision boundary.

¹ <https://github.com/BGT-M/spartan2-tutorials/blob/master/BeatGAN.ipynb>

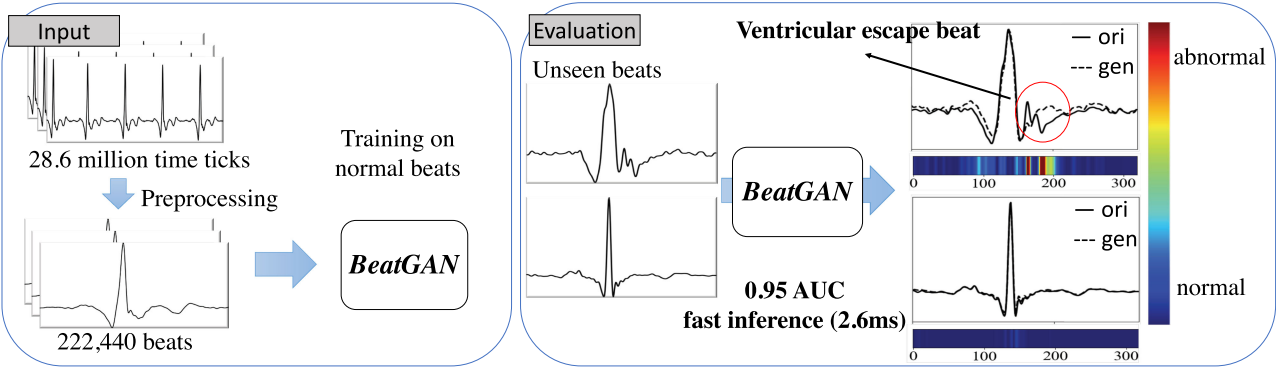


Fig. 2. BeatGAN successfully detects anomalous rhythms, and explains the results. The size of training input is 28.6 million time ticks, and inference can be as fast as 2.6 ms per beat. The original beat is shown by solid lines, and the generated beat is shown by dashed lines.

2.3 Vocabulary-Based Methods

Vocabulary-based methods learn a set of vocabularies (patterns) of the given time series. The rare vocabularies are regarded as anomalies. Hidden Markov Models (HMMs) [14] are classic vocabulary-based method. Variants include DynaMMo [15] which uses Dynamic Bayesian Networks and AutoPlait [16] which uses two-level HMMs. Recent work [17] proposed a vocabulary approach named BEATLEX which performs segmentation and forecasting by optimizing minimum description length (MDL). This model automatically segments the given long time series and summarizes the different patterns as vocabularies, these vocabularies are regarded as the basis of the time series and the rare variables are detected as anomalies. And this model can segment long time series more properly and we can get meaningful subsequences. In addition, Keogh *et al.* introduced an efficient data structure, Matrix Profile [18], based on which the given time series can be effectively clustered for the anomalous patterns. [19] proposed a parameter-free algorithm SKIMP to calculate Matrix Profile faster. NormA [20] elaborately selects some of sequences and build normal behavior models based on MDL principal.

2.4 Reconstruction-Based Methods

Anomalies can be defined as events that deviate significantly from the patterns observed in real data [21]. Thus, many works detect anomalies by computing a synthetic reconstruction of the data and then measuring the deviation between an observed instance and its reconstruction. Principal Component Analysis (PCA) and Singular Value Decomposition (SVD) is the linear reconstruction model. The low-rank decomposition makes the model pays more attention to the “normal” part of the data and the anomalous part is ignored in reconstructed data. Autoencoders can also be used for deep-learning based anomaly detection by inspecting its reconstruction error. And it is more suitable for complex data because of the power of deep learning. Jinwon used autoencoders (AE) and variational autoencoders (VAE) for anomaly detection on several benchmark datasets [2]. Dan also proposed a variational autoencoder based reconstruction model to learn the key features of normal time series, and detect the anomalies using the reconstructed time series [22], [23]. The MSCRED model [24] proposes an autoencoder to reconstruct signature matrix to jointly consider the multi-scale time dependence, robustness and

explainability. The USAD [25] utilizes adversely trained autoencoders to learn data features in an unsupervised way while achieving a high performance.

Recently, with the growing interest in generative adversarial networks, researchers have proposed anomaly detection using adversarial training. AnoGAN [4] and Gandomaly [26] are both originally proposed for anomaly detection on visual data, while ours is designed for a series of real numbers that need robustness against speed variations. AnoGAN needs to learn a latent vector for every input for anomaly detection, which is very time consuming and limits its application. Gandomaly uses an encoder-decoder-encoder structure, and identify the anomalies by comparing the latent representations. Zenati uses the BiGAN model which has the ability of both generating and inferencing to detect anomalies and achieves good performance [27]. Inspired by AnoGAN and LSTM-based generative adversarial network [28], Li proposes the MAD-GAN model for industrial time series anomaly detection, the model consists of an LSTM-based generator and LSTM-based discriminator. Our BeatGAN uses data reconstructions, resulting in a more concise model and better performance for time series data. Meanwhile, BeatGAN can give explainable results with such a reconstruction.

Other approaches proposed tensor decomposition based methods for time series forecasting [29], [30] and detecting anomalies based on the forecast [31], [32]. The Deep Autoencoder Gaussian Mixture Model(DAGMM) [33] combines a deep autoencoder and a gaussian mixture model to model the distribution of time series data. Series2Graph [34] represents subsequences in low-dimensional embeddings and identifies anomalies with varying lengths.

BeatGAN provides an explainable approach combining autoencoders and generative adversarial networks, incorporating the advantages of both models. Table 1 summarizes existing works related to our problem. Only BeatGAN satisfies all the desired characteristics.

3 PROPOSED MODEL

Let $T \in \mathbb{R}^{M \times N}$ be a multivariate time series, which is N time ticks in length, and has M dimensions for each time tick, e.g., reading from M sources. A rhythmic time series T contains sub-series, i.e. beats. For example, a beat in the ECG time series consists of a sequence of a P wave followed by a QRS complex, T, and U waves. We fix the window size for a

TABLE 1
A Comparison of Related Approaches

	PCA/SVD	OCSVM	DAGMM	USAD	AnoGAN	Ganomaly	LSTM-AD	MadGAN	MSCRFD	BeatGAN
Non-linear										
Explains anomalies	✓	✓	✓	✓	✓	✓	✓	✓	✓	✓
Robust	✓			✓	✓	✓	✓	✓	✓	✓
Fast inference	✓	✓	✓	✓		✓	✓	✓	✓	✓
Hyper-parameter free	✓	✓								✓

beat in time series, and beats are denoted as $x \in \mathbb{R}^{M \times L}$, where L is large enough for containing a beat. Zero-padding or sampling can be used for fitting irregular beats in such a window if we know the exact length of each beat.

Most beats in time series are normal in practice, and the amount of beats is massive. Our anomaly detection problem can then be described as follows:

Informal Problem 1 (Anomalous beat detection). Given a collection of multivariate time series beats $\mathcal{X} = \{x_i, i = 1, 2, \dots\}$ with most of beats in the normal class,

- Detect anomalous beats x in a collection of unseen time series,
- Such that they deviate significantly from the reconstructed time series, and can pinpoint anomalous time ticks in x for explanation.

3.1 General Framework

The idea of our model is to detect anomalies by reconstructing their “normal” state. In general, the framework for detecting anomalies based on reconstruction error will have two main components: reconstruction (or generation) model optimization, and anomalousness scoring based on the reconstruction.

The optimization objective for learning the reconstruction model is: for input time series, our model reconstructs a more “normal” time series, the anomaly score can be calculated by comparing the residuals between original time series and reconstructed time series. The general reconstruction-based model’s loss function can be formulated as

$$\begin{aligned} L &= \|X - G(X)\|_2 + R(G) \\ &= \sum_x \|x - G(x)\|_2 + R(G), \end{aligned} \quad (1)$$

where X is a matrix concatenating each beat matrix $x \in \mathcal{X}$ along its columns. $G(\cdot)$ is the reconstructed model, and $R(G)$ is the regularization term for different models.

And the anomalousness score for a beat x is calculated as

$$A(x) = \|x - G(x)\|_2, \quad (2)$$

which summarizes the distance of each time tick between original beat and reconstructed beat. After calculating anomalousness score for each dimension, we select the top-5 dimension with the maximum score as potential root cause to direct users’ attention.

Many reconstruction-based anomaly detection methods can be expressed by this framework, using Eq. (1) as objective and Eq. (2) to calculate the anomalousness score. We

TABLE 2
Unifying the Reconstruction-Based Methods for Anomaly Detection

Method	$G(\cdot)$	$R(G)$
SVD/ fBox	$\sum_{k=1}^p \sigma_k u_k v_k^T$	$\lambda_1 \ I - U^T U\ _2 + \lambda_2 \ I - V^T V\ _2$
AE	$G_D(G_E(x))$	/
VAE	$G_D(G_E(x))$	$\lambda D_{KL}[Q(z x) P(z)]$
BeatGAN	$G_D(G_E(x))$	adversarial regularization

$G(\cdot)$ is the reconstruction function, $R(G)$ is the regularization loss.

list the specific forms of reconstruction-based anomaly detection methods including SVD, AE, VAE, and our BeatGAN in Table 2. The $G(\cdot)$ means the reconstruction function and the $R(G)$ is the regularization loss for reconstruction model optimization. The SVD-based methods reconstruct data using low-rank approximation. u_i and v_i are the i th columns of U and V respectively obtained by singular value decomposition. Moreover, fBox uses the same reconstruction model as SVD, but uses a different anomalousness score which applies a threshold based on percentiles of the reconstructed distribution.

The AE-based and VAE-based methods, and BeatGAN are all neural network based model. They reconstruct data using an encoder network $G_E(\cdot)$ and decoder network $G_D(\cdot)$. While AE-based methods do not have any explicit regularization, VAE-based methods use the KL divergence between the approximate posterior distribution $Q(z|x)$ learned by the encoder, and the prior distribution $P(z)$ of the latent variable z often uses Gaussian distribution. While our BeatGAN uses adversarial regularization in its training process.

We will show in the following how BeatGAN regularizes its reconstruction, taking the benefits from generative adversarial networks (GAN).

Fig. 2 shows the framework of our proposed method. In this example, we preprocess the ECG data and train the model with normal heartbeats. At test time, for each unseen beat x , we feed it into the trained model and obtain the reconstructed beat x' (showed by dashed lines in Fig. 2). By comparing the residuals between x and x' , we capture the anomalies.

3.2 Proposed Model With Adversarial Regularization

As Fig. 3 shows, our adversarial reconstruction framework has three key components: encoder $G_E(\cdot)$, decoder $G_D(\cdot)$, and discriminator $D(\cdot)$.

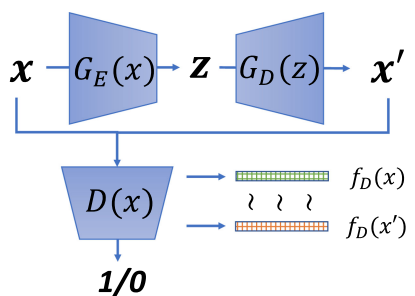


Fig. 3. An illustration of BeatGAN framework.
Authorized licensed use limited to: University of Petroleum & Energy Studies. Downloaded on January 07, 2025 at 03:53:06 UTC from IEEE Xplore. Restrictions apply.

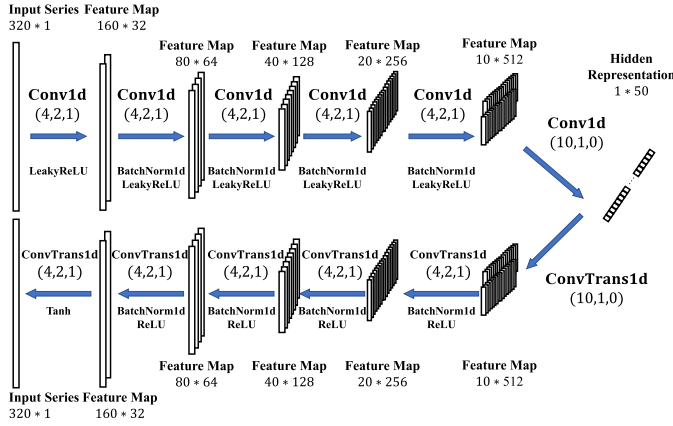


Fig. 4. An illustration of CNN structure in reconstructor (encoder-decoder). Parameters of Conv1d (4,2,1) and ConvTrans1d (4,2,1) mean that the kernel size is 4, the stride is 2 and the padding is 1.

To reconstruct time series x , $G_E(x)$ encodes the input x to a hidden vector z that represents its important features. Then $G_D(z)$ generates a time series x' from the hidden vector z . Thus our reconstruction goal is $G(x) = G_D(G_E(x))$. Discriminator $D(\cdot)$ regularizes the reconstruction by minimizing the classification error.

In the framework, we can generally use the same network structure from a broad range of neural networks. We implement two alternative structures: the one-dimensional convolutional neural network (1-D CNN), and recurrent neural networks (RNN).

1-D CNN. The CNN network is effective in learning good local features (as well as the combinations of them) [35]. So it is more suitable for some medical time series since these time series always contain some sub-patterns [9]. In our proposed model BeatGAN, we use filters in CNN to slide in one dimension along the temporal dimension. The structure of 1-D CNN implemented in encoder is illustrated in Fig. 4.

RNN Networks. Recurrent neural network behaves well on learning the trend of the time series which can be used to handle smoothed time series. We choose the GRU cell as the realization of RNN in our proposed BeatGAN, because GRU cell can avoid the gradient vanishing problem and is more effective than LSTM. GRU cell has two gates: update gate and the reset gate. The cell compute the last hidden state h_t by Eq. (3)

$$\begin{aligned} z_t &= \sigma(W_z \cdot [h_{t-1}; x_t]) \\ r_t &= \sigma(W_r \cdot [h_{t-1}; x_t]) \\ \hat{h}_t &= \tanh(W \cdot [r_t * h_{t-1} +; x_t]) \\ h_t &= (1 - z_t) * h_{t-1} + z_t * \hat{h}_t. \end{aligned} \quad (3)$$

In terms of regularization, we use the adversarial training framework of GAN in our model. In the GAN framework, the generator and the discriminator compete in a two-player min-max game. The discriminator tries to distinguish real beats from reconstructed beats and the generator tries to generate beats that can fool the discriminator. The generator learns the generating mechanism of data by this adversarial training. In the training process, the discriminator $D(\cdot)$ tries to maximize the loss function

$$L_D = \mathbb{E}_{x \sim P_r} [\log D(x)] + \mathbb{E}_{z \sim P_z} [\log (1 - D(G(z)))] \quad (4)$$

which discriminates the generated x' from x as different class label 0 and 1. The generator G tries to minimize the following loss function

$$L_G = \mathbb{E}_{z \sim P_z} [\log (1 - D(G(z)))] \quad (5)$$

which makes the generated beats unable to be discriminated by $D(\cdot)$.

Actually, the essence of generating adversarial networks is to optimize the JS divergence of distribution between real data and the generated data. We get the ideal discriminator D^* when the gradient of L_D equal to 0.

$$D^*(x) = \frac{P_r(x)}{P_r(x) + P_g(x)}. \quad (6)$$

While $P_g(x)$ is the distribution of generated data. And after we use D^* in L_G , we can get the objective function of the generator

$$\begin{aligned} L_G &= \mathbb{E}_{x \sim P_r} [\log D(x)] + \mathbb{E}_{x \sim P_g} [\log (1 - D(x))] \\ &= \mathbb{E}_{x \sim P_r} \left[\log \frac{P_r}{P_r + P_g} \right] + \mathbb{E}_{x \sim P_g} \left[\log \frac{P_g}{P_r + P_g} \right] \\ &= JS(P_r || P_g) - 2\log 2. \end{aligned} \quad (7)$$

In practice, directly using Eq. (5) as adversarial regularization does not perform well due to the diminished gradient and mode collapse, which is also the weakness of the JS divergence. Thus, instead of calculating loss by the original x and vector z in hidden space, we set up the relationship between the original x and reconstructed x' via our reconstruction part of the model. Therefore, we consider using pairwise feature matching loss which minimizes differences of the statistics between original and generated time series, learned in hidden layers of the discriminator $D(\cdot)$. Letting $f_D(\cdot)$ be the activation vector on a hidden layer of the discriminator, pairwise feature matching loss between x and x' is

$$L_{pfm} = \|f_D(x) - f_D(x')\|_2. \quad (8)$$

Overall, the objective of reconstruction with adversarial regularization is to minimize the following loss function:

$$L_G = \|x - x'\|_2 + \lambda \|f_D(x) - f_D(x')\|_2, \quad (9)$$

where $x' = G(x)$, and λ is the weighting parameter adjusting the impact of the adversarial regularization. Meanwhile, the objective of the discriminator is to maximize the following loss function:

$$L_D = \frac{1}{N} \sum_i^N [\log D(x_i) + \log (1 - D(x'_i))]. \quad (10)$$

The discriminator network and the adversarial training process are the biggest differences compared to autoencoders, the adversarial regularization ensures that the reconstruction part will not just compress and decompress the input data.

Finally, we use the Adam optimization algorithm for learning the reconstruction model, as summarized in Algorithm 1.

To perform anomaly detection, we use the reconstruction model to reconstruct a time series x' using our model trained on normal data, for given x . We then evaluate the

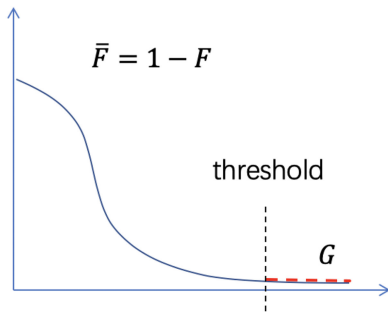


Fig. 5. Fitting data that follows the extremum distribution.

anomalousness score by comparing the difference between x' and x as in Eq. (2). Since anomalies always occur in a portion of time ticks of a beat, the residuals between ticks of x and x' can indicate where the anomaly occurs, routing users' attention to the anomalous portion and providing an explanation.

Algorithm 1. Training Algorithm

```

1:  $\theta_G, \theta_D \leftarrow$  initialize network parameters
2: for number of training iterations do
3:   Sample  $\{x_1, \dots, x_m\} \sim$  a batch from the normal data
4:   Generate  $\{x_1', \dots, x_m'\}$  by  $G_E$  and  $G_D$ 
5:   Compute  $L_D$  by Eq. (10)
6:    $\theta_D \leftarrow \theta_D + \alpha \nabla_{\theta_D}(L_D)$            //  $\nabla$  is the gradient
7:   Compute  $L_G$  by Eq. (9)
8:    $\theta_G \leftarrow \theta_G + \alpha \nabla_{\theta_G}(L_G)$ 
9: end for
```

3.3 Automatic Threshold Selection

During the online anomaly detection, given a multivariate time series with length L , our BeatGAN model computes the anomaly score for each time tick. So the anomaly scores form a univariate time series $\{a_1, a_2, \dots, a_L\}$, our goal is to automatically select the anomalous time ticks. Then the problem can be formed as follows:

Informal Problem 2 (Automatic anomaly detection).

Given a collection of observed normal univariate time series of anomaly score $\{a_1^o, a_2^o, \dots, a_n^o\}$ and a collection of test univariate time series of anomaly score $\{a_1^u, a_2^u, \dots, a_m^u\}$

- Determine whether each time tick in test time series is anomalous (0-normal/1-anomalous)

Here, we use the principle of Extreme Value Theory (EVT) to set a threshold for time tick. Extreme value theory is used to deal with the maximum deviation from the median of probability distribution. So it is often used in the analysis of rare cases (such as once in a century flood and risk analysis in finance). It is more general than other theory because it doesn't need any assumption for data distribution. In EVT, the most widely used is POT (Peaks Over Threshold) theorem, it uses the GPD (Generalized Pareto Distribution) to estimate the extremum (value greater than a certain threshold) distribution. Like Fig. 5 shows, we will use GPD (red dash line) to fit the data larger than threshold.

The idea of POT is to fit the tail portion of the data distribution with GPD with parameter σ, γ [36]

$$f(x) = \frac{1}{\sigma} \left(1 + \frac{\gamma x}{\sigma} \right)^{-\frac{1}{\gamma}}.$$

For parameter σ and γ , we can estimate the value by Maximum Likelihood Estimation(MLE), then we can set the threshold with another risk parameter q ,

$$z = t + \frac{\sigma}{\gamma} \left(\left(\frac{qn}{N_t} \right)^{-\gamma} - 1 \right). \quad (11)$$

The automatic threshold selection algorithm is summarized in Algorithm 2, it is also a streaming algorithm. The algorithm will only store the data that is larger than the given threshold, so it only occupies little memory. For each streaming data, the algorithm will compare it with the current anomaly threshold, if it is larger than the anomaly threshold, this data will be stored in the anomalies set. Otherwise, the algorithm will re-estimate the current Generalized Pareto distribution and compute another anomaly threshold. So in this algorithm, the anomaly thresholds change over time.

Algorithm 2. Anomaly Detection

```

Input: parameter  $q$ 
1:  $A \leftarrow \emptyset$ 
2:  $th \leftarrow$  initial threshold
3:  $Y = \{a_i^o - th | a_i^o > th\}$ 
4:  $\gamma, \sigma \leftarrow MLE(Y)$ 
5:  $z_q = CalThreshold(q, \gamma, \sigma, k, |Y|, th)$            // by Eq. (11)
6:  $k \leftarrow n$ 
7: for  $i > 0$  do
8:   if  $a_i^u > z_q$  then
9:     Add( $a_i^u$ ) in A
10:   else if  $a_i^u > th$  then
11:     Add  $i$  in Y
12:      $\gamma, \sigma \leftarrow MLE(Y)$ 
13:      $z_q = CalThreshold(q, \gamma, \sigma, k, |Y|, th)$            // by Eq. (11)
14:   else
15:      $k \leftarrow k + 1$ 
16:   end if
17: end for
```

3.4 Data Augmentation Using Time Warping

For the time series similarity measure, euclidean Distance is mainly used in many applications since it is simple and effective. While there is another special similarity measure, named dynamic time warping (DTW) [37]. DTW can compare the "shape" of two time series more accurately and it measures similarity in a way that is more robust against variations in speed (i.e., 'time warping'). For example, heartbeats naturally and slightly speed up or slow down. However, since DTW is not differentiable, we cannot directly use it for reconstruction error in objective Eq. (9). [38] proposed a variation of DTW called SoftDTW which can be used to calculate the similarity of time series. We use such method to replace the euclidean Distance to calculate the loss of reconstruction as:

$$L_G = SoftDTW(x, x') + \lambda \cdot SoftDTW(f_D(x), f_D(x')). \quad (12)$$

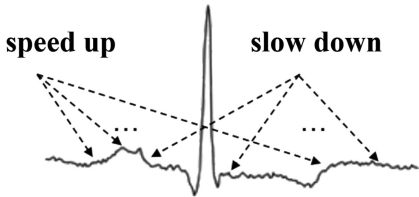


Fig. 6. Data Augmentation by a modified time warping method. "Speed up" means that we randomly sample k_1 time ticks and delete their values, "slow down" means that we randomly sample k_2 time ticks and insert the average value of their two adjacent time ticks before the sampled time ticks.

Furthermore, we propose a modified time warping for data augmentation to make our model robust against natural variability involving time warping in real time series. As shown in Fig. 6, we augment our training data as follows. For each training beat x , we sample uniformly at random a small number k_1 of time ticks to "slow down" and a different k_2 time ticks to "speed up" to keep the fixed length of time series. For each time tick to "speed up", we will directly delete the data value at that time tick. While for each time tick to "slow down", we will insert a new data value just before that time tick, whose value is set to the average of the data values at the 2 adjacent time ticks. This results in a modified version of x , which we use as additional training data for our model.

4 EXPERIMENT

In this section, we will design different experiments to answer the following questions:

Q1. Accuracy. How accurately does our method find out anomalies compared with other baselines?

Q2. Robustness. How robust can our model achieve with data augmentation?

Q3. Explainability. How well does BeatGAN pinpoint anomalous portions of input time series, and route people's attention?

Q4. Efficiency. How fast does BeatGAN test on samples compare with other GAN-based baselines?

Q5. Sensitivity. How sensitive does BeatGAN for amplitude and frequency changes? What is the performance of BeatGAN on controlled synthetic time series?

4.1 Data

We evaluate our proposed model on ECG time series from MIT-BIH Arrhythmia Database² [39], sensor time series from SWaT database.³ And we use motion capture data from the CMU motion capture database⁴ to do case study to show the explainability of our method. The datasets are listed in Table 4.

MIT-BIH ECG dataset. The MIT-BIH arrhythmia dataset contains 48 ECG records from test subjects from Beth Israel Hospital. The ground-truth labels are annotated on the R-peak of each beat by two or more independent cardiologists indicating positions and types of each heartbeat. As recommended by the AAMI [40], the normal beats include the beats annotated with labels N, L, and R,⁵ and the records

named 102, 104, 107, and 218 are removed due to insufficient signal quality. In total, the dataset contains 97,568 beats and 28.6 million time ticks. In experiments, we augment the data and normalize them between -1 and 1 by min-max scaling.

SWaT dataset The secure water treatment system(SWaT) dataset [41] is collected from a six-stage Secure Water Treatment system. The testbed is designed for representing a large water refreshing plant which can refresh 5 gallons water per minute in modern cities. Based on this testbed, we can simulate two state modes: normal and abnormal. A total of 25 dimensions which record readings of sensors are regarded as input dimensions. Generally, this dataset is divided into train and test sections. The former section contains 496,800 samples collected in the first several days with no anomalies at all, while 449,919 samples are recorded in the latter section to simulate anomalies. In experiments, we normalize each time series x between -1 and 1 by min-max scaling.

CMU Motion Capture dataset. The dataset contains motion-captured subjects performing different motions (walking, jogging, running, etc.). We choose 4 dimensions from different sensors on the subject's body, i.e. left-right arms and legs. We select 16 walking records of 6,616 ticks in total, 10 jogging records of 1,608 ticks in total, and 1 jumping record of 2,085 ticks for training and testing separately. Thus we obtain 10,309 time ticks in total. In experiments, we normalize each time series x between -1 and 1 by min-max scaling.

4.2 Accuracy

BeatGAN calculates the anomalousness score for each time tick of a beat. Given an evaluation set \mathcal{Z} , BeatGAN calculates the score of beat s_i in different ways for different models and forms a score set S , i.e. $S = \{s_i : A(x_i), x_i \in \mathcal{Z}\}$. For the ECG set, we average the scores of each time tick as score of the beat. For SWaT dataset, we treat the last time tick as the anomalousness score of the whole "beat". To calculate metrics, we first standardize the scores between 0 and 1 by min-max scaling.

$$s'_i = \frac{s_i - \min(S)}{\max(S) - \min(S)}.$$

Then we calculate the two metrics, AUC (Area Under ROC Curve) and Best F1 score. For AUC metric, we first compute the ROC curve for the model and AUC is calculated as the area under the curve. For Best F1 score, we will enumerate each threshold of scores in test dataset and compute the corresponding F1 score. Then we select the highest F1 score among them as our Best F1 score metric.

We compare the performance with PCA-based method, one-class SVM (OCSVM) [13] for anomalous class (using the top 50 features selected by PCA method). DAGMM [33] is a density based model which combine the autoencoder and gaussian mixture model. USAD [25] uses autoencoder structure with adversarial learning to isolate anomalies. AnoGAN [4] is a deep convolutional generative adversarial network and Ganoomaly [26] utilizes a conditional generative adversarial network to reconstruct. Besides, we choose LSTMAD and MAD-GAN as baselines of BeatGAN(RNN). LSTMAD is an LSTM-based AutoEncoder [42]. The model MAD-GAN uses the framework of AnoGAN, and replaces

2. <https://physionet.org/content/mitdb/1.0.0/>

3. https://itrust.sutd.edu.sg/itrust-labs_datasets/dataset_info/

4. <http://mocap.cs.cmu.edu/>

5. N is Normal beat, L is Left bundle branch block beat and R is Right bundle branch block beat.

TABLE 3
Results of MIT-BIH ECG Dataset and SWaT Dataset

Method	MIT-BIH ECG		SWaT	
	Best-F1 score	AUC score	Best-F1 score	AUC score
PCA	0.7087 ± 0.0047	0.8164 ± 0.0037	0.7731 ± 0.0011	0.8222 ± 0.0023
OCSVM	0.6759 ± 0.0019	0.7917 ± 0.0018	0.2761 ± 0.0042	0.6336 ± 0.0031
DAGMM	0.6769 ± 0.0005	0.6999 ± 0.0002	0.7848 ± 0.0012	0.7324 ± 0.0001
USAD	0.3837 ± 0.0001	0.3521 ± 0.0001	0.6365 ± 0.0002	0.7901 ± 0.0002
AnoGAN	0.7091 ± 0.0074	0.8642 ± 0.0100	0.7556 ± 0.0023	0.7792 ± 0.0021
Ganomaly	0.7708 ± 0.0187	0.9083 ± 0.0122	0.7557 ± 0.0025	0.8115 ± 0.0090
LSTMAD	0.7105 ± 0.0013	0.5960 ± 0.0008	0.7632 ± 0.0039	0.8148 ± 0.0044
MadGAN	--	--	0.77	--
MSCRED	0.7783 ± 0.0000	0.6273 ± 0.0002	0.5960 ± 0.0029	0.7466 ± 0.0003
BeatGAN(CNN)	0.8159 ± 0.0102	0.9447 ± 0.0053	0.7814 ± 0.0020	0.8192 ± 0.0031
BeatGAN(RNN)	0.6910 ± 0.0233	0.8361 ± 0.0307	0.7838 ± 0.0023	0.8185 ± 0.0033

the underlying convolutional network with LSTM network. In Table 3, we directly use the result of SWaT reported in this paper [43]. Finally, we also compare with MSCRED [24], which employs a convolutional encoder-decoder and attention-based ConvLSTM network to perform anomaly detection task.

4.2.1 Evaluation on ECG Dataset

Experimental Setup. We first use a filter [44] to remove the noise in ECG sequences. We choose 320 time ticks as the window size for a beat: 140 time ticks before the given R-peak and 180 ticks after it. We set the dimension size of latent space as 50, $\lambda = 1.0$ for objective (9). The structure of G_D learns the architecture of the generator from DCGAN [45]. We use 5 1D transposed convolutional layers followed by batch-norm and leaky ReLU activation, with slope of the leak set to 0.2. The transposed convolutional kernel's size and number of each layer are 512(10/1)-256(4/2)-128(4/2)-64(4/2)-32(4/2): e.g., 512(10/1) means that the number of filters is 512, the size of filter is 10 and the stride is 1. G_E 's structure is a mirrored version of G_D and D has the same architectural details as G_E , which is shown in Fig. 4. We also design the RNN-based BeatGAN model, we choose GRU as the underlying cell, the hidden units are set as 50 and the number of layer is 1. We use Adam optimizer with an initial learning rate $lr = 0.0001$, and momentums $\beta_1 = 0.5$, $\beta_2 = 0.999$. Moreover, we use 5-fold cross-validation for each method, and report the averaged metrics and standard deviations (std).

Result. As shown in Table 3, the averaged results and std of the non-linear methods generally have better performance in both AUC and Best F1 as compared to PCA and OCSVM, providing evidence that non-linear models have advantages on the complex ECG time series. Besides, The

results show that BeatGAN(CNN) perform the best among the baselines ($p\text{-value} < 0.01$). From the Table 3 and Fig. 8, we can also notice that the BeatGAN(RNN) perform much worse than BeatGAN(CNN), the reason maybe that the convolutional neural network is more effective in learning good local features (as well as the combinations of them) [35] since the ECG time series contains many patterns, like P waves, QRS complex and T waves. And so the 1-D CNN is widely used in many ECG time series [9], [46].

We also design the experiment to verify the performance of the automatic threshold selection algorithm. Here we select the $3 - \sigma$ rule as the baseline, the $3 - \sigma$ rule detects the anomalies as following:

- assume the distribution of the anomaly score is Gaussian.
- compute the parameters the the Gaussian distribution μ and σ
- for each test anomaly score, if it is higher than $\mu + 3\sigma$, then regards it as anomaly

For MIT-BIH dataset, we set the parameter $q = 0.04$ and the initial threshold th as 98% percentile. The result is shown in Fig. 9, we can find out that our algorithm can achieve the better performance than baseline, and the final F1 score is only little lower than the best F1 score, which means it is suitable for the real-world task.

4.2.2 Evaluation on SWaT Dataset

Experimental Setup. For SWaT dataset, since the anomalies only occur at the end of the time series, we naturally split the training part and the testing part (the data collected during the first seven days is training data and the data collected during the last four days is testing data). We first down-sample to original time series to one measurement every 5 seconds, then normalize the multivariate time series to $[-1, 1]$ by min-max scale. We slide a window of 60 time ticks along the original multivariate time series to generate the segments, the stride size is 1 tick. Since the annotated label is located at each time tick, we use the reconstruction error of last time tick as the anomaly score for this "beat". The dimension size of latent space is 20 and $\lambda = 0.1$. We use both the 1-D CNN based model and RNN-based model to do the experiments. For decoder G_D of 1-D CNN based BeatGAN model, we use 4 1D transposed convolutional layers followed by batch-norm and

TABLE 4
The Description of Datasets

Dataset	dimension	size (time tick)	anomalous ratio
MIT-BIH	1	28.6 M	11.1
SWaT	25	946 K	5.8
CMU Motion	4	10.3 K	--

Anomalous ratio is the percentage of anomalous data in total data.

Authorized licensed use limited to: University of Petroleum & Energy Studies. Downloaded on January 07, 2025 at 03:53:06 UTC from IEEE Xplore. Restrictions apply.

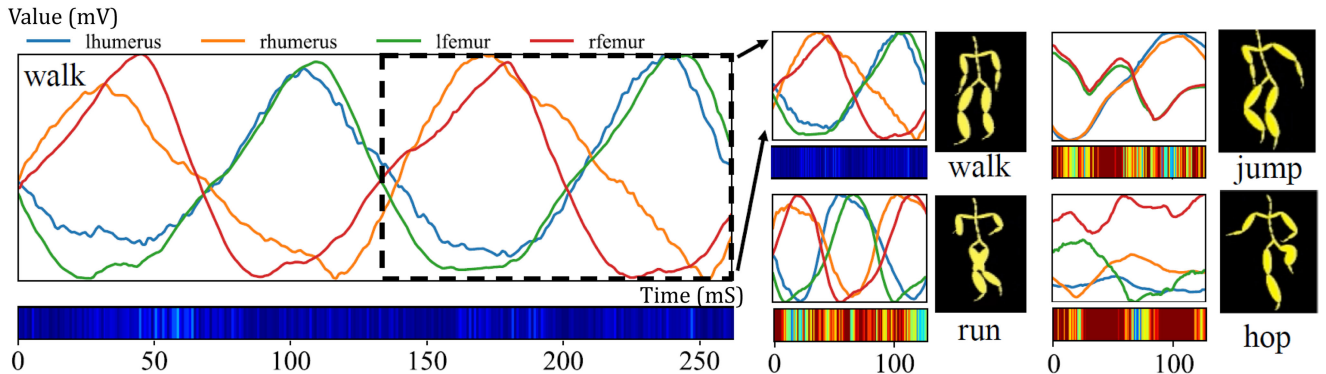


Fig. 7. An example of anomaly detection on motion capture time series(4-dimensions). The right side shows the original time series and heatmaps pinpoint the anomalies of jumping/running/hopping from walking motions.

leaky ReLU activation, with a slope of the leak set to 0.2. The transposed convolutional kernel's size and the number of each layer are 256(4/1)-128(4/2)-64(4/2)-32(4/2): e.g., 256(4/1) means that the number of filters is 256, the size of the filter is 4 and the stride is 1. G_E 's structure is a mirrored version of G_D and D has the same architectural details as G_E . As for RNN-based BeatGAN model, we also choose the GRU cell since it is more concise and effective, the hidden units are set as 20 and the number of layer is 1. The learning rate of the Adam optimizer is 0.001, we test each model with 5 runs and give the mean and std. The result is listed in Table 3.

Result. In the experiment of SWaT dataset, we also compare different baselines. From Table 3, we can find out that BeatGAN model achieves a high best F1 score, outperforming other baselines except the DAGMM. Because of the more simple pattern in SWaT dataset, the PCA model can also achieve a high AUC and Best F1, and both CNN-based BeatGAN model and RNN-based BeatGAN model have good performance. The performance of One Class SVM is worst and the reason may be that the dimension of the time series is too high. While other models can have good performance in this anomaly detection task.

Then we also test the performance of the automatic threshold selection algorithm compared to the baseline: $3 - \sigma$ rule. For SWaT dataset, we set the parameter $q = 0.1$ and the initial threshold th as 98% percentile. The result is shown in Fig. 9, we can also find that our algorithm performs better than the baseline, and it proves the algorithm is suitable for general tasks.

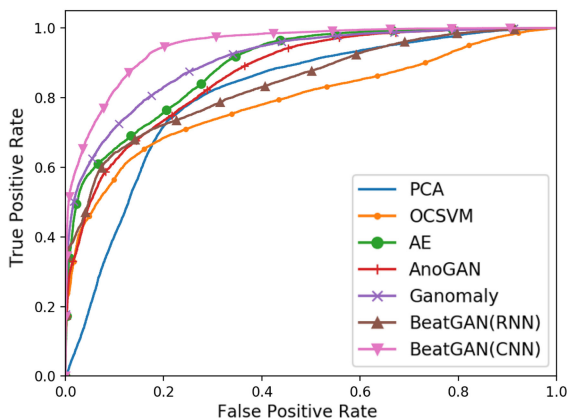


Fig. 8. The ROC curve of different model for MIT-BIH dataset.

Authorized licensed use limited to: University of Petroleum & Energy Studies. Downloaded on January 07, 2025 at 03:53:06 UTC from IEEE Xplore. Restrictions apply.

4.2.3 Case Study on Motion Capture Dataset

Experimental Setup. In this experiment, walking is considered as our normal class. We evaluate BeatGAN on detecting unusual motions of jogging and jumping time series. We slide a window of 64 time ticks along the original multivariate time series to generate beats, and the stride size for the sliding window is 5 ticks. Thus we obtain 1,729 beats, with 10,309 time ticks in total, some of which overlap. Since the data is sparse and small, we test the performance of the RNN-based BeatGAN model for the study case. We use the GRU cell with 10 neural units and 1 layer. The dimension size of latent space is 10 and $\lambda = 0.01$.

Result. Fig. 10 shows the histogram of normalized anomalousness scores on evaluation data. The results show that the score distributions of walking and others are clearly separated (red represents the anomalousness scores of walk and blue represents others), which means our BeatGAN can perfectly discriminate between unusual motions (jogging/jumping) and usual motions (walking), by only using time series of walking for training.

4.3 Data Augmentation and Robustness

In this part, we will test our model to investigate the effectiveness and robustness of the data augmentation strategy. We test the data augmentation strategy on the ECG dataset, and we set $k = 16$ for data augmentation. The result of data augmentation is shown in Fig. 11. In this experiment, all BeatGAN models are based on 1D-CNN. And the BeatGAN (aug) means we augment the training data size to $3 \times$ with time warping strategy. For BeatGAN*(aug), we add the 0.1% anomalous time series to the training data for evaluating

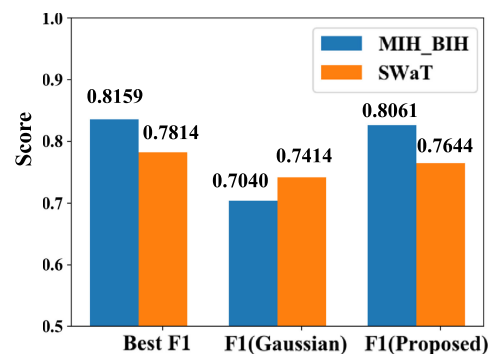


Fig. 9. The result of automatic threshold selection algorithm.

Authorized licensed use limited to: University of Petroleum & Energy Studies. Downloaded on January 07, 2025 at 03:53:06 UTC from IEEE Xplore. Restrictions apply.

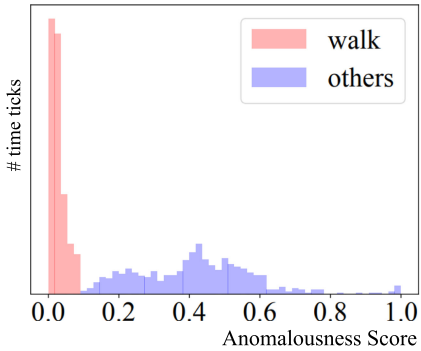


Fig. 10. Normalized anomalousness score distributions of walking and others.

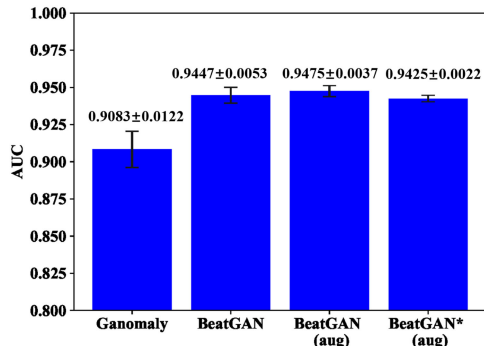


Fig. 11. The performance of BeatGAN with data augmentation.

robustness. The result shows our data augmentation strategy can slightly improve the AUC score of BeatGAN model. Besides, as shown in Fig. 12, with little anomalies(2% - 10%) in training data, the performance of our BeatGAN model will drop slightly which also shows the robustness of the model.

[38] modifies DTW and makes it a differentiable algorithm that can replace the MSE loss in Eq. (9). We use BeatGAN CNN model to verify its effectiveness. BeatGAN (softdtw-softdtw) stands for replacing MSE loss with SoftDTW loss for both reconstruction error and adversarial regularization. And BeatGAN(softdtw-mse) stands for only replacing the error of reconstruction. BeatGAN(mse-mse) is the same as BeatGAN(CNN) in Table 3. The results shown in Table 5 demonstrate that the SoftDTW-based model performs slightly worse than the MSE-based model while both of them outperform other baselines. Furthermore, the lower standard error shows greater stability of SoftDTW-based loss which can be utilized more in the future.

4.4 Explainability

Next, we show that BeatGAN can pinpoint the time ticks when the anomalous pattern occurs. In the right part of Fig. 2, we compute the residual for each time tick between input beat and generated beat: $res(t) = (x(t) - x'(t))^2$ at time t , and show the heatmap of residual values. As we observe, our model gives high anomalousness scores for the abnormal beat (top right) and low anomalousness scores for the normal beat (bottom right). This abnormal beat is a ‘ventricular escape beat’ and our model correctly identifies that the abnormal time ticks occur in its QRS complex (circled region). Besides, our model generates the “normal” generated beat (dashed lines), which provides additional

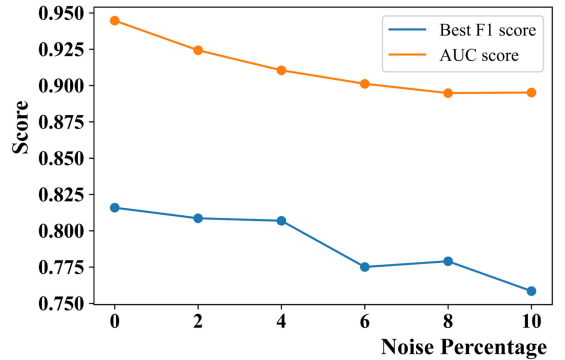


Fig. 12. The performance degradation of BeatGAN with noised data.

TABLE 5
Results of Soft-DTW and MSE Loss

Method	Best F1 Score	AUC Score
BeatGAN(softdtw-softdtw)	0.7841 ± 0.0009	0.9215 ± 0.0003
BeatGAN(softdtw-mse)	0.7844 ± 0.0009	0.9223 ± 0.0002
BeatGAN(mse-mse)	0.8159 ± 0.0102	0.9447 ± 0.0053

explainability by allowing users to compare the generated beat to the observed beat, to understand how the observed beat differs.

In Fig. 7, the left time series is the record of walking. On the right, we illustrate the results of a jogging, jumping or hopping time series, using a heatmap whose color indicates the size of the residual at each time tick. We compute the residual for each time tick by $res(t) = \max(x(t) - x'(t))^2$, where $x(t)$ is a 4-dimensional vector at time t , and max takes the max value over the 4 dimensions, which we use as the anomalousness score of time tick t . The heatmap shows that BeatGAN cannot well reconstruct the time series of jogging/jumping/hopping, thus correctly assigning them high anomalousness, since we only use walking time series for training.

Besides, we also visualize the reconstruction results to see what the model learns. In Fig. 13, we show the reconstruction samples of walking, running and hopping time series. The Fig. 13a shows the reconstruction example of the walking time series where left is the original input time series. We can see that the model can reconstruct this walking time series well, resulting in a low anomalousness score. And for Figs. 13b and 13c, the reconstruction examples of running and hopping time series are shown. For running time series (left picture in Fig. 13b), it has the high frequency compare to walking time series(left picture in Fig. 13a), while the reconstructed time series is more like “walking” state, leading to a high anomalousness score and so for the hopping time series. From these, we may find out that our model can reconstruct the input time serise as more “normal” time series and this is in line with our expectations.

4.5 Efficiency

To verify the efficiency of the BeatGAN, We ran the inferences of BeatGAN, AnoGAN and Ganomaly, which are all based on generative adversarial network. We run the experiment on a server with a Tesla K80 GPU using ECG dataset. Downloaded on January 07,2025 at 03:53:06 UTC from IEEE Xplore. Restrictions apply.

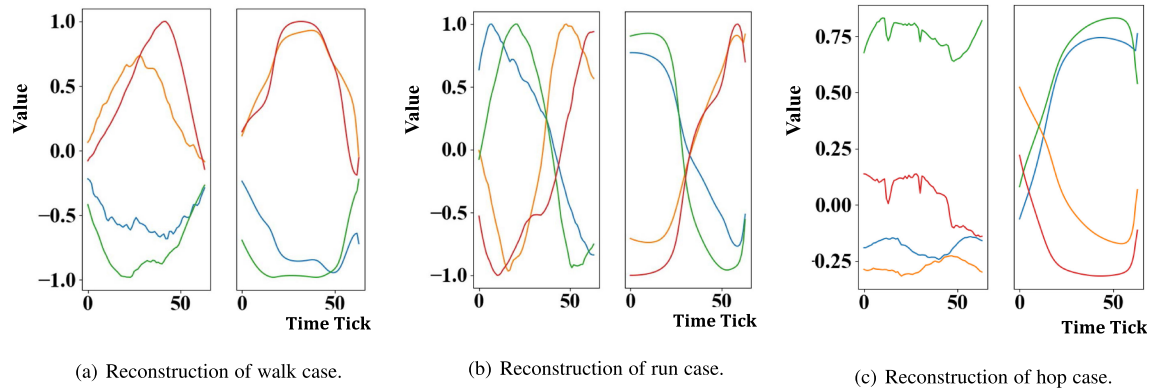


Fig. 13. Reconstruction samples on 4-dimension time series of captured motions. (Left is the input time series, right is the reconstructed time series).

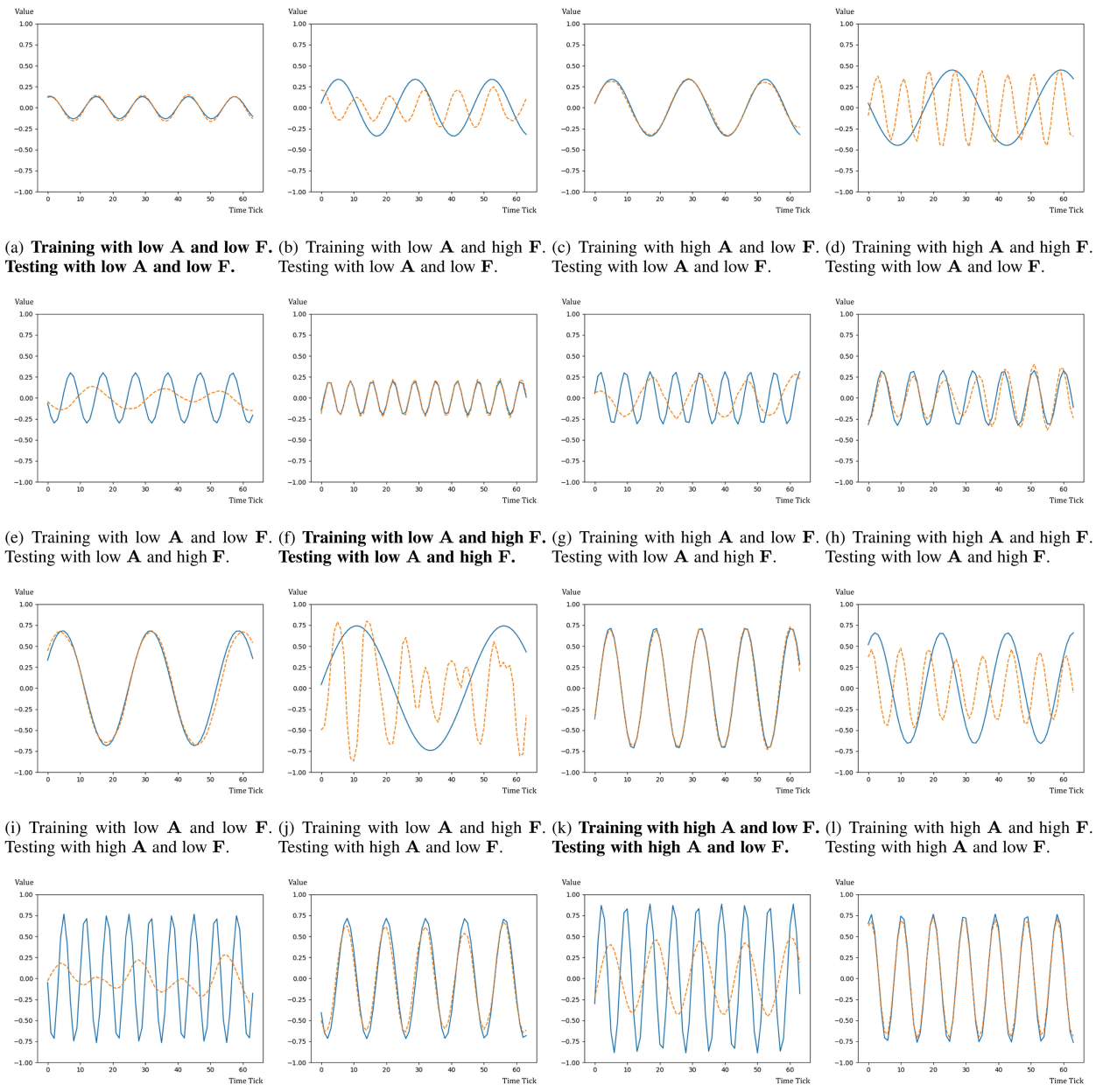


Fig. 14. Reconstruction samples on synthetic sine waves. The original time series is plotted by solid lines, and the reconstruction is plotted by dashed lines. **A** and **F** are amplitudes and frequencies respectively. The cases with bold captions are trained and tested by the time series of similar amplitudes and frequencies.

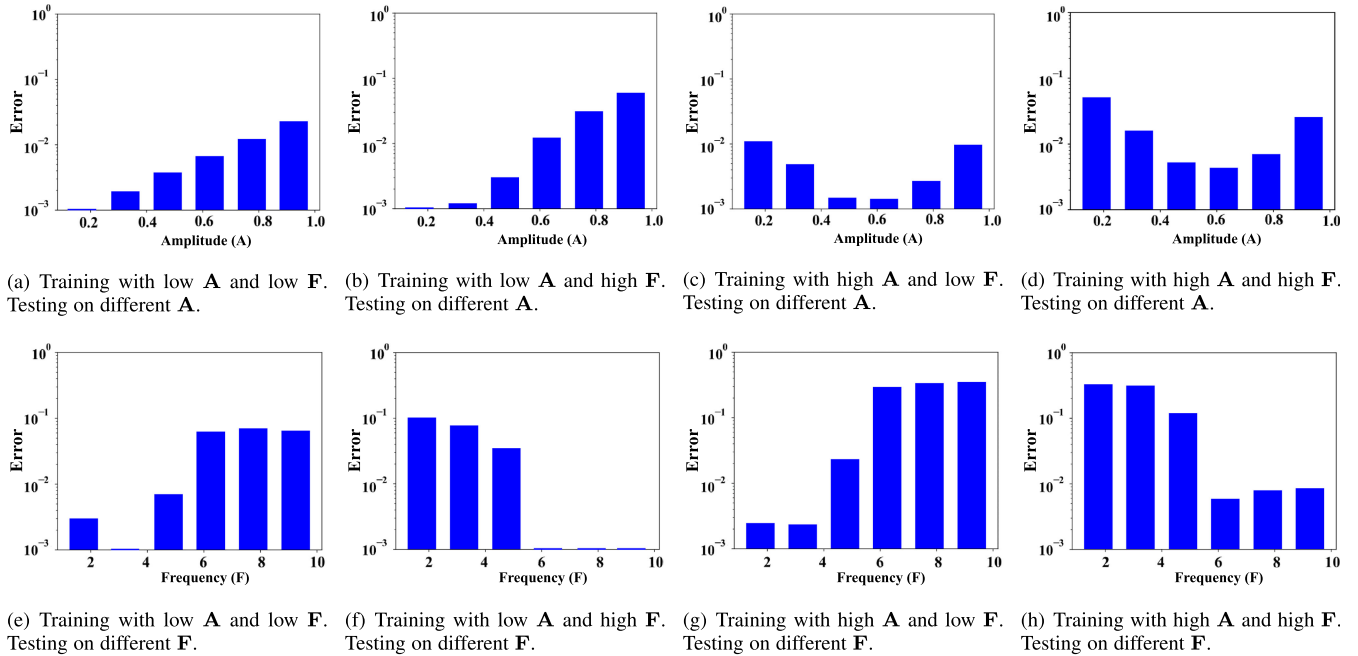


Fig. 15. Mean reconstruction errors of training and testing on various amplitudes (A) and frequencies (F).

Three models are all implemented in PyTorch. Besides, we set the iteration number of AnoGAN as 500 as in [4].

Fig. 16 (the *y*-axis is a logarithmic scale) shows that BeatGAN only takes 2.6 ms per beat, which is 1.5× faster than Gandomaly and 1415× faster than AnoGAN. Actually, BeatGAN is fast for inference at test time since the adversarial generation of BeatGAN is one-pass through the feed-forward neural network. In contrast, the baseline AnoGAN is a two-step anomaly detection model. AnoGAN needs an extra step to find the corresponding latent vector for the given time series by iterative computation, so it is slowest in the test phase. While the model Gandomaly is also end-to-end but it has another encoder network which is more complex compared with BeatGAN.

4.6 Sensitivity Experiments on Synthetic Dataset

To further understand the ability of our BeatGAN model, we test the model with 1D-CNN as its implementation on the synthetic time series. We generate the sine waves as our toy data. There are two main parameters for sine waves: amplitude and frequency. We create our training dataset with various amplitudes and frequencies, i.e., low amplitudes randomly in (0.1, 0.5), high amplitudes randomly in

(0.5, 0.9); low frequencies randomly in (1.0, 5.0) and high frequencies randomly in (5.0, 10), where (*a*, *b*) means any real number larger than *a* and less than *b*.

So we have 4 combinations for our training dataset to train our model. For testing, we want to know how well BeatGAN can reconstruct the sine time series with various parameters, i.e. amplitudes, and frequencies. Figs. 14a, 14b, 14c, 14d, 14e, 14f, 14g, 14h, 14i, 14j, 14k, 14l, 14m, 14n, 14o, and 14p shows the different reconstruction examples with different models. In the first column of figures, the model is trained by time series of low amplitude and low frequency and tested separately on time series of low amplitude and low frequency, low amplitude, and high frequency, high amplitude and low frequency, and high amplitude, and high frequency. The second column of figures shows the results of the model which is trained by time series of low amplitude and high frequency. And the 3rd and 4th columns are illustrated as such. From these figures, we can see that BeatGAN reconstructs well with various amplitudes and similar frequencies. But BeatGAN is sensitive to frequency, which reconstructions deviate further away from the originals if the training and testing time series have quite different frequencies. In another word, the model can reconstruct well even the amplitude of test sample is not observed (higher or lower) in training time series, while the model reconstruct poorly if the frequency of the test sample is not seen in training.

We also design the quantitative experiments to support this idea. Fig. 15 shows the quantitative result. The first row shows the mean reconstruction error with amplitude changes of different models and the second row shows the mean reconstruction error with frequency changes of different models. The first column shows the result of model trained by low amplitude and low frequency, the second column shows the model trained by low amplitude and high frequency, the third column shows the model trained by high amplitude and low frequency, and the fourth shows the model trained by high

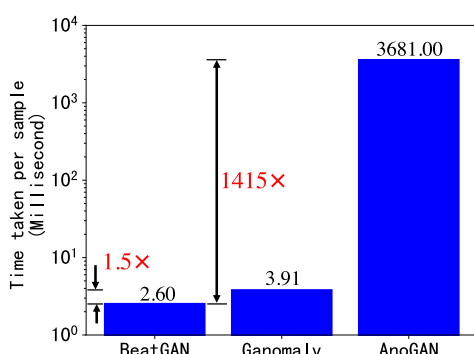


Fig. 16. BeatGAN has fast inference (2.6 ms).

amplitude and high frequency. Note that the y -axis is a logarithmic scale. We can find out that the mean reconstruction error is more steady while the mean reconstruction error changes much more when frequency changes. The low reconstruction error may mean the model regards the test samples are generated from same mechanism as its training data while high reconstruction error means the high probability of different generation mechanism. This phenomenon reveals that the model may not actually learn the sine function and the complex pattern like frequency is hard to learn.

5 CONCLUSION

We propose a reconstruction based model with automatic threshold selection algorithm for time series anomaly detection. The model detects anomalies using the adversarially generated time series. For underlying structure, we design both the 1D CNN based and the RNN based neural network, while the CNN based model is more suitable for medical waveforms and the RNN based model is more suitable for smoothed waveforms. In conclusion, our model has the following advantages:

- Unsupervised: BeatGAN is the reconstruction based anomaly detection model. It detects anomalies by observing massive normal time series.
- Effectiveness: BeatGAN outperforms baselines in both accuracy and inference speed, achieving high accuracy in three datasets and very fast inference.
- Explainability: BeatGAN can pinpoint the anomalous ticks to route people's attention as shown in Fig. 2;
- Generality: BeatGAN can also successfully detect anomalies in many time series from different domains.

ACKNOWLEDGMENTS

This is an extension of the original conference paper: B. Zhou et al, BeatGAN: Anomalous Rhythm Detection using Adversarially Generated Time Series, IJCAI-19.

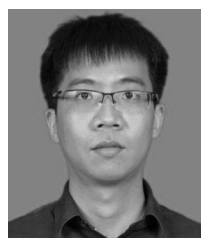
REFERENCES

- [1] N. Shah, A. Beutel, B. Gallagher, and C. Faloutsos, "Spotting suspicious link behavior with fbox: An adversarial perspective," in *Proc. IEEE Int. Conf. Data Mining*, 2014, pp. 959–964.
- [2] J. An and S. Cho, "Variational autoencoder based anomaly detection using reconstruction probability," *Special Lecture IE*, vol. 2, pp. 1–18, 2015.
- [3] I. Goodfellow et al., "Generative adversarial nets," in *Proc. Adv. Neural Inf. Process. Syst.*, 2014, pp. 2672–2680.
- [4] T. Schlegl, P. Seeböck, S. M. Waldstein, U. Schmidt-Erfurth, and G. Langs, "Unsupervised anomaly detection with generative adversarial networks to guide marker discovery," in *Proc. Int. Conf. Inf. Process. Med. Imag.*, 2017, pp. 146–157.
- [5] V. Chandola, A. Banerjee, and V. Kumar, "Anomaly detection: A survey," *ACM Comput. Surv.*, vol. 41, no. 3, pp. 1–58, 2009.
- [6] F. E. Grubbs et al., "Sample criteria for testing outlying observations," *Ann. Math. Statist.*, vol. 21, no. 1, pp. 27–58, 1950.
- [7] A. Siffer, P.-A. Fouque, A. Termier, and C. Largouet, "Anomaly detection in streams with extreme value theory," in *Proc. 23rd ACM SIGKDD Int. Conf. Knowl. Discov. Data Mining*, 2017, pp. 1067–1075.
- [8] B. Hooi, K. Shin, H. Lamba, and C. Faloutsos, "TelTail: Fast scoring and detection of dense subgraphs," in *Proc. 34th AAAI Conf. Artif. Intell.*, 2020, pp. 4150–4157.
- [9] P. Rajpurkar, A. Y. Hannun, M. Haghpanahi, C. Bourn, and A. Y. Ng, "Cardiologist-level arrhythmia detection with convolutional neural networks," 2017, *arXiv:1707.01836*.
- [10] S. Kiranyaz, T. Ince, and M. Gabbouj, "Real-time patient-specific ECG classification by 1-D convolutional neural networks," *IEEE Trans. Biomed. Eng.*, vol. 63, no. 3, pp. 664–675, Mar. 2016.
- [11] Y. Shen, M. Voisin, A. Aliamiri, A. Avati, A. Hannun, and A. Ng, "Ambulatory atrial fibrillation monitoring using wearable photoplethysmography with deep learning," in *Proc. 25th ACM SIGKDD Int. Conf. Knowl. Discov. Data Mining*, 2019, pp. 1909–1916.
- [12] Y. Roh, G. Heo, and S. E. Whang, "A survey on data collection for machine learning: A Big Data-ai integration perspective," *IEEE Trans. Knowl. Data Eng.*, vol. 33, no. 4, pp. 1328–1347, Apr. 2021.
- [13] B. Schölkopf, R. C. Williamson, A. J. Smola, J. Shawe-Taylor, and J. C. Platt, "Support vector method for novelty detection," in *Proc. Adv. Neural Inf. Process. Syst.*, 2000, pp. 582–588.
- [14] L. E. Baum and T. Petrie, "Statistical inference for probabilistic functions of finite state Markov chains," *Ann. Math. Statist.*, vol. 37, no. 6, pp. 1554–1563, 1966.
- [15] L. Li, J. McCann, N. S. Pollard, and C. Faloutsos, "DynaMMo: Mining and summarization of coevolving sequences with missing values," in *Proc. 15th ACM SIGKDD Int. Conf. Knowl. Discov. Data Mining*, 2009, pp. 507–516.
- [16] Y. Matsubara, Y. Sakurai, and C. Faloutsos, "AutoPlait: Automatic mining of co-evolving time sequences," in *Proc. ACM SIGMOD Int. Conf. Manage. Data*, 2014, pp. 193–204.
- [17] B. Hooi, S. Liu, A. Smalagic, and C. Faloutsos, "BEATLEX: Summarizing and forecasting time series with patterns," in *Proc. Joint Eur. Conf. Mach. Learn. Knowl. Discov. Databases*, 2017, pp. 3–19.
- [18] C.-C. M. Yeh et al., "Matrix Profile I: All pairs similarity joins for time series: A unifying view that includes motifs, discords and shapelets," in *Proc. IEEE 16th Int. Conf. Data Mining*, 2016, pp. 1317–1322.
- [19] F. Madrid, S. Imani, R. Mercer, Z. Zimmerman, N. Shakibay, and E. Keogh, "Matrix profile XX: Finding and visualizing time series motifs of all lengths using the matrix profile," in *Proc. IEEE Int. Conf. Big Knowl.*, 2019, pp. 175–182.
- [20] P. Boniol, M. Linardi, F. Roncalli, T. Palpanas, M. Meftah, and E. Remy, "Unsupervised and scalable subsequence anomaly detection in large data series," *VLDB J.*, vol. 30, pp. 909–931, 2021.
- [21] D. M. Hawkins, *Identification of Outliers*, vol. 11. Berlin, Germany: Springer, 1980.
- [22] H. Xu et al., "Unsupervised anomaly detection via variational auto-encoder for seasonal KPIs in web applications," in *Proc. World Wide Web Conf.*, 2018, pp. 187–196.
- [23] Y. Su, Y. Zhao, C. Niu, R. Liu, W. Sun, and D. Pei, "Robust anomaly detection for multivariate time series through stochastic recurrent neural network," in *Proc. 25th ACM SIGKDD Int. Conf. Knowl. Discov. Data Mining*, 2019, pp. 2828–2837.
- [24] C. Zhang et al., "A deep neural network for unsupervised anomaly detection and diagnosis in multivariate time series data," in *Proc. AAAI Conf. Artif. Intell.*, 2019, pp. 1409–1416.
- [25] J. Audibert, P. Michiardi, F. Guyard, S. Marti, and M. A. Zuluaga, "USAD: Unsupervised anomaly detection on multivariate time series," in *Proc. 26th ACM SIGKDD Int. Conf. Knowl. Discov. Data Mining*, 2020, pp. 3395–3404.
- [26] S. Akcay, A. Atapour-Abarghouei, and T. P. Breckon, "Ganomaly: Semi-supervised anomaly detection via adversarial training," 2018, *arXiv:1805.06725*.
- [27] H. Zenati, C. S. Foo, B. Lecouat, G. Manek, and V. R. Chandrasekhar, "Efficient GAN-based anomaly detection," 2018, *arXiv:1802.06222*.
- [28] H. Arnelid, E. L. Zec, and N. Mohammadha, "Recurrent conditional generative adversarial networks for autonomous driving sensor modelling," in *Proc. IEEE Intell. Transp. Syst. Conf.*, 2019, pp. 1613–1618.
- [29] H. A. Song, B. Hooi, M. Jereminov, A. Pandey, L. Pileggi, and C. Faloutsos, "PowerCast: Mining and forecasting power grid sequences," in *Proc. Joint Eur. Conf. Mach. Learn. Knowl. Discov. Databases*, 2017, pp. 606–621.
- [30] B. Hooi, H. A. Song, A. Pandey, M. Jereminov, L. Pileggi, and C. Faloutsos, "StreamCast: Fast and online mining of power grid time sequences," in *Proc. SIAM Int. Conf. Data Mining*, 2018, pp. 531–539.
- [31] P. Chen, S. Liu, C. Shi, B. Hooi, B. Wang, and X. Cheng, "NeuCast: Seasonal neural forecast of power grid time series," in *Proc. 27th Int. Joint Conf. Artif. Intell.*, 2018, pp. 3315–3321.
- [32] B. Hooi, K. Shin, S. Liu, and C. Faloutsos, "SMF: Drift-aware matrix factorization with seasonal patterns," in *Proc. SIAM Int. Conf. Data Mining*, 2019, pp. 621–629.

- [33] B. Zong *et al.*, "Deep autoencoding Gaussian mixture model for unsupervised anomaly detection," in *Proc. Int. Conf. Learn. Representations*, 2018, pp. 1–19.
- [34] P. Boniol and T. Palpanas, "Series2Graph: Graph-based subsequence anomaly detection for time series," *Proc. VLDB Endowment*, vol. 13, no. 12, pp. 1821–1834, 2020.
- [35] L. Guo, G. Sim, and B. Matuszewski, "Inter-patient ecg classification with convolutional and recurrent neural networks," *Biocybernetics Biomed. Eng.*, vol. 39, no. 3, pp. 868–879, 2019.
- [36] J. Jocković, "Quantile estimation for the generalized pareto distribution with application to finance," *Yugoslav J. Operations Res.*, vol. 22, no. 2, pp. 297–311, 2016.
- [37] T. K. Vintsyuk, "Speech discrimination by dynamic programming," *Cybern. Syst. Anal.*, vol. 4, no. 1, pp. 52–57, 1968.
- [38] M. Cuturi and M. Blondel, "Soft-DTW: A differentiable loss function for time-series," in *Proc. 34th Int. Conf. Mach. Learn.*, 2017, pp. 894–903.
- [39] G. B. Moody and R. G. Mark, "The impact of the MIT-BIH arrhythmia database," *IEEE Eng. Med. Biol. Mag.*, vol. 20, no. 3, pp. 45–50, May/Jun. 2001.
- [40] "American national standard for testing and reporting performance results of cardiac rhythm and ST segment measurement algorithms," *AAMI/ANSI Standard EC57*, 1998.
- [41] A. P. Mathur and N. O. Tippenhauer, "SWaT: A water treatment testbed for research and training on ics security," in *Proc. Int. Workshop Cyber-Phys. Syst. Smart Water Netw.*, 2016, pp. 31–36.
- [42] P. Malhotra, A. Ramakrishnan, G. Anand, L. Vig, P. Agarwal, and G. Shroff, "LSTM-based encoder-decoder for multi-sensor anomaly detection," 2016, *arXiv:1607.00148*.
- [43] D. Li, D. Chen, L. Shi, B. Jin, J. Goh, and S.-K. N. Mad-gan, "Multivariate anomaly detection for time series data with generative adversarial networks," 2019, *arXiv:1901.04997*.
- [44] C. Carreiras *et al.*, "BioSPPy: Biosignal processing in python," 2015, Accessed: Jan. 12, 2019. [Online]. Available: <https://github.com/PIA-Group/BioSPPy/>
- [45] A. Radford, L. Metz, and S. Chintala, "Unsupervised representation learning with deep convolutional generative adversarial networks," 2015, *arXiv:1511.06434*.
- [46] S. Hong, Y. Zhou, J. Shang, C. Xiao, and J. Sun, "Opportunities and challenges in deep learning methods on electrocardiogram data: A systematic review," 2019, *arXiv:2001.01550*.



Shenghua Liu received the PhD degree from the Computer Science and Technology Department, Tsinghua University. He is an associate professor with the Institute of Computing Technology, Chinese Academy of Sciences. He once visited with the University of California, Los Angeles and visited with Carnegie Mellon University as a research scholar respectively. His current research interests include big graph mining, time series analysis, spectral graph theory, and anomaly detection. Two of the related papers have been recognized as "Best Paper" Award and candidate.



Bin Zhou received the master's degree from the Institute of Computing Technology, University of Chinese Academy of Sciences, in 2020. His research interests include time series mining and machine learning.



Quan Ding received the BS degree from NanKai University, in 2020. He is currently working toward the master's degree with the University of Chinese Academy of Sciences. His main research interests are time series mining and machine learning.



Bryan Hooi received the PhD degree in machine learning from Carnegie Mellon University. He is an assistant professor with the School of Computing and the Institute of Data Science in National University of Singapore. His research interests include scalable machine learning, deep learning, graph algorithms, anomaly detection, and biomedical applications of AI.



Zhengbo Zhang received the PhD degree from the Institute of Medical Equipment, Academy of Military Medical Sciences. He is an associate professor with the Center for Artificial Intelligence in Medicine, Chinese PLA General Hospital. He was a visiting scientist with the Laboratory for Computational Physiology, Massachusetts Institute of Technology, and Center for Dynamical Biomarkers with Beth Israel Deaconess Medical Center / Harvard Medical School respectively. His current research interests are secondary analysis of electronic health records, predictive analysis of physiological time series, and application of wearable physiological monitoring systems, Internet of Things, and Artificial Intelligence in clinical scenario.



Huawei Shen received the PhD degree from the Institute of Computing Technology, in 2010. He is a professor with the Institute of Computing Technology, Chinese Academy of Sciences (CAS). His major research interests include network science, social media analytics, and recommendation. He has published more than 80 papers in prestigious journals and top international conferences, including in *Science*, *PNAS*, *Physical Review E*, *WWW*, *AAAI*, *IJCAI*, *SIGIR*, *CIKM*, and *WSDM*. He is an outstanding member of the Association of Innovation Promotion for Youth of CAS. He received the Top 100 Doctoral Thesis Award of CAS, in 2011 and the Grand Scholarship of the President of CAS, in 2010.



Xueqi Cheng is a professor with the Institute of Computing Technology, Chinese Academy of Sciences (ICT-CAS), and the director of the Research Center of Web Data Science & Engineering (WDSE) in ICT-CAS. His main research interests include network science etc. He has published more than 100 publications in prestigious journals and conferences, including *IEEE Transactions on Knowledge and Data Engineering*, *Physical Review E*, *SIGIR*, *WWW* etc.

▷ For more information on this or any other computing topic, please visit our Digital Library at www.computer.org/csdl.